A CCHP system based on ORC cogenerator and adsorption chiller experimental prototypes: Energy and economic analysis for NZEB applications

A CCHP system based on ORC cogenerator and adsorption chiller experimental prototypes: energy and economic analysis for NZEB applications

Walter Lombardo[a,b], Alessio Sapienza[a*], Saverio Ottaviano[b], Lisa Branchini[b], Andrea De Pascale[b], Salvatore Vasta[a]

[a] CNR-ITAE – Institute of Advanced Energy Technologies "Nicola Giordano", Messina, Italy

[b] DIN – Alma Mater Studiorum, University of Bologna, Bologna, Italy

*Corresponding author: tel. +39.090.624229, fax +39.090.624247, e-mail address: alessio.sapienza@itae.cnr.it

ABSTRACT

In this work, the study of a novel solar driven Combined Cooling, Heating and Power (CCHP) system is carried out. In particular, the system is composed of a 60 m^2 flat plate solar thermal collectors field, a 10 kW_e photovoltaic plant, a 2 m^3 Thermal Energy Storage (TES), a 3 kW_e micro-Organic Rankine Cycle (micro-ORC) prototype, a 4.4 kW_c thermally driven Adsorption Chiller (AC) coupled with a 6 kW_c auxiliary Heat Pump (HP). It has been conceived for residential applications and has been integrated with a real bioclimatic nearly zero energy building (NZEB). The building-plant system has been modelled in TRNSYS environment and studied for three Italian locations, spread along the peninsula, with three different climates, Messina, Milano and Rome. An energy, environmental and economic analysis have been carried out. The system has been assessed on hourly basis and the sensitivity analysis has demonstrated that performances are sensitive to location. In particular, the effectiveness of the system is greatly affected by solar radiation and weather condition. The CCHP system works for about 2400 hours during the whole year on average with global efficiencies ranging from 32% to 42%. The plant is generally suitable for air conditioning applications in residential sector only with a government's financial support. A medium value of Pay Back Time of 6 years has been found with a medium Net Present Value of 50 kEUR. In conclusion, this study has highlighted the potential of solar driven micro-CCHP systems based on advances technologies for residential applications.

KEYWORDS

CCHP, NZEB, ORC, Adsorption Chiller, Dynamic simulation, HVAC

NOMENCLATURE

CCHP	Combined Cooling, Heating And Power
NZEB	Nearly Zero Energy Building
SHP	Separate Heat and Power
ORC	Organic Rankine Cycle
AC	Adsorption Chiller
HP	Heat Pump
TES	Thermal Energy Storage
ICE	Internal Combustion Engine
HVAC	Heating, Ventilation, And Air Conditioning
ACP	Average Cooling Power, kW
SCP	Specific Cooling Power, kW/kg
VCP	Volumetric Cooling Power, kW/m^3
S/V	Surface to volume ratio, m^{-1}
S	Net floor area, m^2
s	Thickness, m
U	Stationary thermal transmittance, W/m^2 K
U_g	Glass thermal transmittance, W/m^2 K
U_f	Frame thermal transmittance, W/m^2 K
HDD	Heating daily Degree Days
FPC	Flat Plate Collectors
PV	Photovoltaic
A	Area of the collectors, m^2
c_p	Specific heat, J/kg K
P_e	Electric power, kWe
Q_c	Cooling Power, kWc
Q_{th}	Thermal Power, kWt
E	Annual energy, kWh
I	Solar radiation, W/m^2
$\dot{m}$	Mass flow rate. kg/h
$\dot{V}$	Volumetric flow rate, m^3/h
t	Time, s
h	Hour
h_n	Specific enthalpy at point n of the cycle, kJ/kg K
T	Temperature, °C
T_{TES}	Average temperature of the TES, °C
SPB	Simple Pay Back Period, y
COP	Coefficient Of Performance
PES	Primary Energy Saving
NPV	Net Present Value
GWP	Global Warming Potential
FESR	Fuel Energy Saving Ratio
IC	Investment Cost, EUR
f_{CO2}	Italian CO_2 emission factor, kg_{CO2}/kWh
Subscripts	
a	Ambient
m	Mechanical
el	Electrical
in	Inlet
out	Outlet
c	Cooling
h	Heating
exp	Expander
iso	Isentropic

p	Pump
Rec	Recuperator
SH	Superheating degree
L	Low
M	Medium
H	High
glob	global
Greek Symbols	
ρ	Density, kg/m^3
η	Efficiency

INTRODUCTION

In the last years, the increasing global energy demand and, thus, the energy-related environment pollution, has led to looking for new strategies in several sectors including manufacturing, transports, buildings, services. In 2017, according to the International Energy Agency (IEA) annual report about energy efficiency, the 20% of the global energy demand is related to the residential sector [1]. Furthermore, energy demand about the air conditioning has been assessed as the 65% of residential sector requirements [2]. In Europe, application of EU Directives on energy efficiency has significantly improved the energy performance of new constructions with the concept of Zero Energy Building (ZEB). In particular, the goal is all new buildings have to satisfy the requirements of nearly zero-energy building (NZEB) by 2021 [3]. Several studies have been carried out on this topic. Ascione et al. investigated in [4] different solutions for the optimization of NZEB buildings in Mediterranean climate. The study has been based on a multi-objective analysis. In [5] and [6] authors investigated novel energy efficiency strategies for developing NZEBs considering a combination of energy efficiency, economic and environmental impact indicators. Different solutions to supply NZEB buildings in different locations have been analysed in [7].

Nowadays, also Combined Heating and Power (CHP) and Combined Cooling, Heating and Power (CCHP) systems in residential sector can be a solution for the achievement of EU strategies. These systems have been demonstrated to offer a technical and economical alternative to traditional Separate Heat and Power (SHP) systems and the simultaneous production of heating, cooling and electric energy can improve the global energy efficiency [8]. In this context, the optimization of CHP systems represents the main challenge in order to minimize the primary energy consumption and CO_2 emissions [9,10]. In [11], different CCHP systems have been analyzed in order to reach the best configuration in order to reducing the primary energy consumption. According to results, absorption chillers can be a promising alternative to conventional refrigeration systems even though compression chillers generally assure a higher COP value. Cardona et al. studied Hybrid CCHP systems with a power-to-heat ratio capable to follow the building demand [12]. In [13], authors investigated a micro-CHP system in different climates and demonstrated its suitability for different loads of end-users buildings with the thermal load sharing approach.

CCHP systems supplied by geothermal heat source and using ejector transcritical CO_2 and Rankine cycles have been studied in [14]. Di Wu et al. proposed a thermodynamic study of an innovative solar driven CCHP system integrated ORC. Results showed a primary energy ratio of 60.2% [15].

Therefore, low enthalpy ORC systems, absorption or adsorption chillers and other systems capable to work with low-grade heat to produce electricity and cooling power become attractive because they can be supplied by thermal energy from renewable sources and/or waste heat. They have limited electricity and fuel consumption in order to achieve a cost and CO_2 emissions reduction. Concerning ORC systems, their development in small scale cogeneration plants for residential application is still a challenge for researchers, as discussed in [16]. Garcia-Saez et al. investigated regarding a solar-driven ORC based CHP compared with a solar reversible heat pump under several operating modes and scenarios and presented an energetic and economic analysis. The Net Present Value (NPV) can be positive by this kind of systems under certain climate conditions [17]. A CCHP desiccant-based air handling unit has been simulated on TRNSYS environment by authors in [18]. A thermo-economic analysis has been carried out showing promising results.

About refrigeration demand, the current use of vapour compression systems involves the employment of refrigerants with an high Global Warming Potential (GWP). To comply with the

international strategies on energy efficiency, a promising alternative is represented by thermally driven systems, since they can be supplied with waste heat, for example coming from Internal Combustion Engines (ICEs), or with renewable source like solar thermal collectors, to produce refrigeration energy [19].
In such a context, adsorption systems represent a promising choice since they can be operated by low grade heat source (i.e. T<100 °C) and employ zero GWP/natural refrigerants like water, alcohols and ammonia [19]. Many examples exist about research activities devoted to the development of adsorption systems. In [20] a silica gel-water adsorption chiller for solar cooling has been investigated by means of a complex mathematical model. The study demonstrated the feasibility of solar-driven adsorption cooling for optimization and primary energy saving purposes. Xia et al. presented a silica gel-methanol adsorption chiller for application in HVAC systems, having SCP of 0.2 kW/kg with a COP of 0.5 [21]. In [22], authors developed a novel silica gel-water adsorption chiller tested with driving temperatures even lower than 60 °C and performances of 3.6 kW cooling power and 0.32 COP, with a volumetric cooling power of 3 kW/m^3, have been obtained. Many advancements have been achieved also through the development of new components and materials in order to reduce the volume and increase the energy density. In [23] authors investigated modified adsorbents with particular properties, for heat pumping, air conditioning and refrigeration applications. Vasta et al. studied a new family of zeolite coatings on graphite plates in order to develope new advanced adsorbers [24]. A novel prototype using AQSOA FAM Z02/water as working pair has been designed, realized and characterized in [25]. Dynamic behaviours of AQSOA zeolites-water working pairs have been investigated also in [26]. Selection criteria of innovative coated bed constructions of adsorbent beds have been discussed by authors in [27], in order to increase the heat and mass transfer. Saeed et al. analysed last findings of this research field on a recent review about desiccant coated heat exchanges [28]. Adsorption systems have been designed also for other applications. In particular, an innovative cooling system for automotive application was modelled and validated with experimental data. The obtained results showed the maximum cooling power achieved at 10 °C (35 °C of condensation temperature) was up to 5 kW with a COP of 0.6 [29]. Another example of adsorption system for mobile air-conditioning has been realized at CNR – ITAE and integrated in a real truck cabin (IVECO STRALIS). The prototype consists of a double-bed adsorber connected with an evaporator and a condenser and supplied by the waste thermal energy from the engine. The system is able to achieve an Average Cooling Power (ACP) = 1÷2.3 kW and a Cooling COP = 0.25÷0.45, at nominal operating conditions [30]. Commercial adsorption chillers for building air conditioning and industrial applications are already available in the market. Invensor [31] and Fahrenheit [32] are the major European producers of cooling systems with a nominal capacity ranging between 30 kW and 300 kW.
In this context, the aim of this work is to study the integration of an ORC cogeneration system with an adsorption chiller in a trigenerative configuration coupled with an innovative bioclimatic building to achieve the concept of NZEB building. The studied CCHP system has been modelled in TRNSYS and is based on ORC and adsorption chiller prototypes developed and experimentally tested respectively at the University of Bologna and at the CNR-ITAE of Messina. The main peculiarities of the ORC system under investigation, widely described in [33] and recalled in [34], are: i) very low heat source temperature (between 60 °C and 90 °C), that makes the system suitable for poor heat sources, like flat plate solar collectors or shallow geothermal wells; ii) low power output (0-3 kW), being appropriate for supplying the electric demand of residential users; iii) the expansion machine, which is a prototype of reciprocating piston model, made of three cylinders with a star configuration. A similar expander with four cylinders, developed for similar power output range [35], is currently employed in a micro-ORC power plant coupled with a low temperature (< 60 °C) geothermal well. The system works with R134a, being suitable for hot source temperature lower than 90 °C, and it is conceived for the

residential sector. The Adsorption Chiller unit (AC) is a prototype designed and realized at CNR-ITAE of Messina and is featured by a novel configuration based on adsorbers with hybrid coated/granular adsorbent beds. An advanced management strategy has been employed with different periods of the isobaric ads/desorption steps under real HVAC operating conditions. The adsorption chiller is fully described by authors in [36,37].
The experimental campaigns previously conducted to draw a complete performance map, of the ORC and AC prototypes by the use of dedicated lab scale test benches was used to simulate the real working conditions of the CCHP system.
The paper represents a prosecution of the activity resumed in [38] where the thermodynamic analysis of the CCHP plant is presented. This work regards the application for a residential end-user and the evaluation of energy, environmental and economic performances.

1. CASE STUDY

1.1 The building

The studied building, shown in Fig.1, is a single-family detached house located in Linguaglossa, a small town in the Metropolitan City Area of Catania (South Italy), with a net conditioned area of around 251.2 m^2. The surface to volume ratio (S/V) is equal to 0.13. The location is in the D climatic zone with heating degree days (HDD) equal to 1760, according to classification specified by the Italian legislative decree 412/93 [39]. The winter period is considered from November 1st to April 15th. It has been designed as a bioclimatic house in a way that allows occupants to benefit from natural advantages of its site and, nowadays, it's a typical example of high efficiency building characterized by maximum thermal comfort and energy saving.
The solutions selected for building envelope takes into account new interesting wooden made materials. The external and internal walls are made of a larch slab insulated with an air layer and mineral wool wood panels. They also are covered with gypsum fibreboards. Roof and floor are wooden made too and insulated with woodfibre boards.


a)

b)

Figure 1. Building (a) North and (b) South views [40]

The building is provided with different-sized windows with double-glazing low emissivity and aluminium frames with thermal break. Thermal properties of windows are described below in Table 1, while Table 2 reports thermal properties for different opaque surfaces of the building envelope.

Table 1. Thermo-physical parameters for windows

Parameter	Value
Glass thermal transmittance, U_g	2.320 W/m^{2}K
Frame thermal transmittance, U_f	3.7 W/m^{2}K
Thermal resistance of the shading, $R_{shading}$	0.3 m^{2}K/W
Total thermal transmittance, U_{tot}	1.479 W/m^{2}K

Table 2. Main characteristics of the building envelope

Building	Total transmittance [W/m^{2}K]	Thickness [m]
External walls	0.318	0.4
Internal walls	1.22	0.36
Roof	0.332	0.25
Floor	0.047	0.81
Windows	1.479	-

1.2 The CCHP plant

Fig. 2 shows the concept layout of the coupled ORC-AC system in tri-generative arrangement. The prototype plant under analysis consists of: a 60 m^2 flat plate solar thermal collectors plant, a 10 kW_e photovoltaic solar plant, a 3 kW_e Organic Rankine Cycle power unit, a 4.4 kW_c adsorption chiller and an auxiliary 6 kW_c reversible heat pump. A 2 m^3 thermal energy storage (TES) is used as heat buffer, which is provided with electro-resistances as supplementary thermal source, and fan coils as terminals for the distribution system. The size of the auxiliary Heat Pump is chosen on the basis of the thermal and cooling loads of the buildings. If the thermal power available from AC system is not enough to meet the load, additional heating or cooling power is supplied by the Heat Pump with a nominal seasonal COP_h of 4, during the heating period, and a nominal seasonal COP_c of 3 in the cooling period. Flow rates of ORC-AC and distribution circuits have been fixed depending on the location, thus on the variability of thermal and cooling demands of the building. Considering available technologies, the hydronic air-conditioning system is the most suitable and it was considered for both heating and cooling periods for the proposed application. The input water temperature to the fan coils has been fixed at 40 °C and 10 °C during heating and cooling period respectively. The features of the main components of the system are summarized in Table 3:

Table 3. Characteristics of the main components

Design specifications	Value
Solar collectors area	60 m^2
PV peak electric power	10 kW_e
ORC system nominal capacity	3 kW_e
Adsorption chiller nominal capacity	4.4 kW_c
Heat Pump nominal capacity	6 kW_c
TES volume	2 m^3

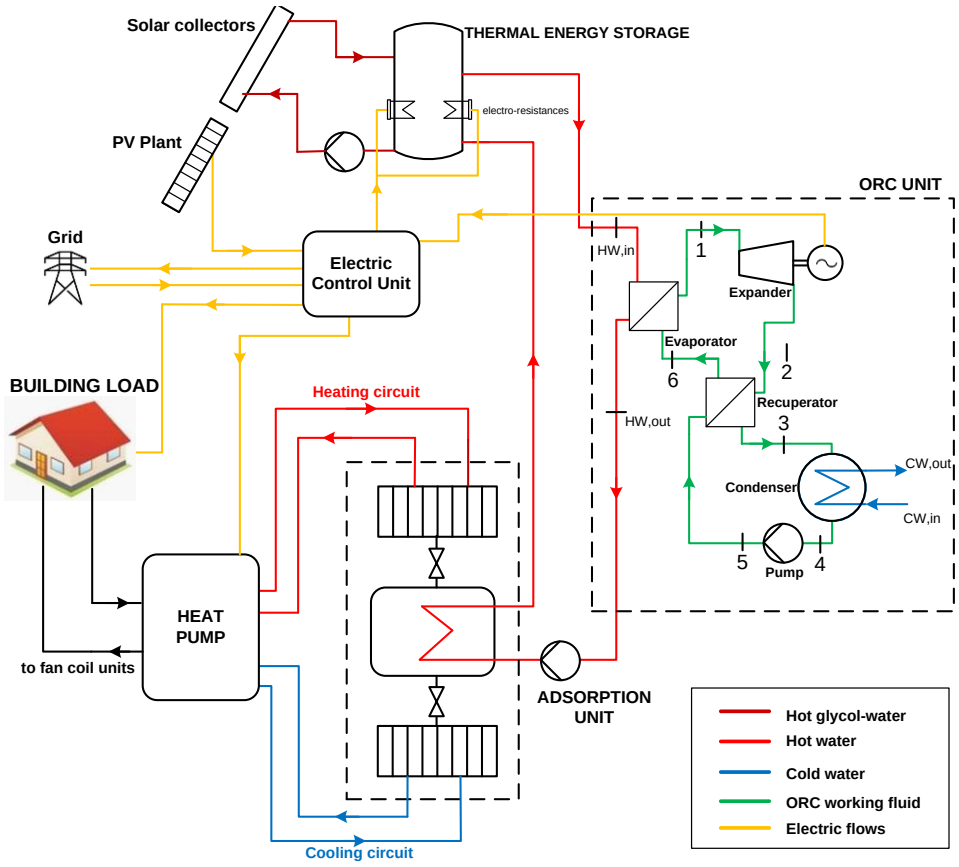

Fig. 2 Schematic layout of the Micro CCHP system and Electric power flow diagram

The thermal solar field heats up the water stored in a 2 m^3 thermal energy storages interacting with ORC-AC circuit. The circulation pump of the solar circuit is operated when the outlet water temperature from solar collectors exceeds the tank average temperature.
The tank is insulated with a material of thermal loss coefficient equal to 0.54 W/m2 K. The water inside TES is kept over 68 °C during CCHP operating hours in order to supply the ORC unit. If the temperature inside the TES is lower than 68 °C, also the auxiliary electric resistances are turned on in order to keep the water temperature in the required range. The water, leaving the ORC, supplies the AC unit in series with the ORC. During winter, the AC works as a heat pump in order to keep the supply temperature to the fan coils at 40 °C. In summer, the chiller mode is turned on to keep the supply temperature to the fan coils at 10 °C. The operating strategy is based on following the thermal loads while electrical energy available from ORC and PV plant is mainly used to meet the electric load of the building and to drive the auxiliaries of the plant. If the electric production is not enough to meet the load, the needed part is drawn from the grid. Instead, if the "production" exceeds the demand, the surplus electricity is fed into grid. The electronic control unit works in order to balance the electric power.

The ORC power unit, shown in Fig. 3a, consists of a recuperated cycle using R134a as working fluid and is rated for a maximum power output of 3 kWe. The system has been produced by the company StarEngine and it was conceived for being supplied by a heat source temperature between 60 °C and 90 °C, with a concept designed for the residential sector. The plant is driven by a reciprocating piston expander made of three radial cylinders placed a 120° and coupled with a permanent magnet generator. The other components of the prototype are two brazed plate heat

exchangers as evaporator and recuperator, a shell and tube condenser and an external gear pump. Main specifications of the ORC system are collected in Table 4, while more details can be found on patent document [41] and on previous publications [33,34]. The full experimental characterization of the plant has been described by authors in [33]. The plant behaviour has been evaluated in the range of hot source temperature between 65 °C and 85 °C, varying the working fluid flow rate, obtained with the control of the feed pump rotating frequency, and evaporation pressure. The experimental data obtained during the test campaign have been used to obtain the trends of the main operating variables of the plant, which are introduced in the semi-empirical model for governing the micro-ORC system behaviour.

Table 4. Main specifics of the micro-ORC system [33,34]

Micro-ORC system specification	Value
Thermal input	15-40 kW
Max hot source temperature	90 °C
Electric power output	0-3 kW
Cooling system	Water-cooled
Working fluid	HFC-134a
Dimensions (l x l x h)	800 mm x 850 mm x 2200 mm
Fluid charge	18-20 kg

The adsorption chiller used in the simulation, shown in Fig. 3b, has been developed at CNR-ITAE. The adsorption chiller works with a ratio between the adsorption and desorption duration equal to 2. This innovative management strategy is possible thanks to an architecture with three adsorbers connected to single evaporator and condenser by pneumatic vacuum valves. The Average Cooling Power (ACP) delivered from the chiller is 4.4 kW_c under nominal boundary conditions (T_H = 90 °C, T_L = 18 °C and T_M = 25 °C) with a Volumetric Cooling Power (VCP) of 9.36 kW/m^3 and COP 0.35. The Adsorber-Heat Exchanger (Ad-HEx) layout is highly performing with customized aluminum finned flat tubes heat exchangers, high specific heat transfer surface area, and is compact, lightweight and to be able to host a good amount of sorbent material. The Ad-HExs have an hybrid configuration because fins were coated with the Mitsubishi AQSOA FAM Z02 sorbent [42] and, then, embedded with Microporous Silica Gel loose grains [43] [44]. Water was selected as refrigerant. The complete description of the adsorption chiller and detailed operation features of the testing procedures can be found in [36,37].
The main characteristics of AC prototype are depicted in Table 5:

Table 5. Characteristics of the main components and operating conditions

Adsorption Chiller specifications	Value
Nominal ACP	4.4 kW
Nominal VCP	9.36 kW/m^3
Nominal COP	0.35
Dimensions	860 mm× 790 mm × 690 mm
Volume	0.47 m^3

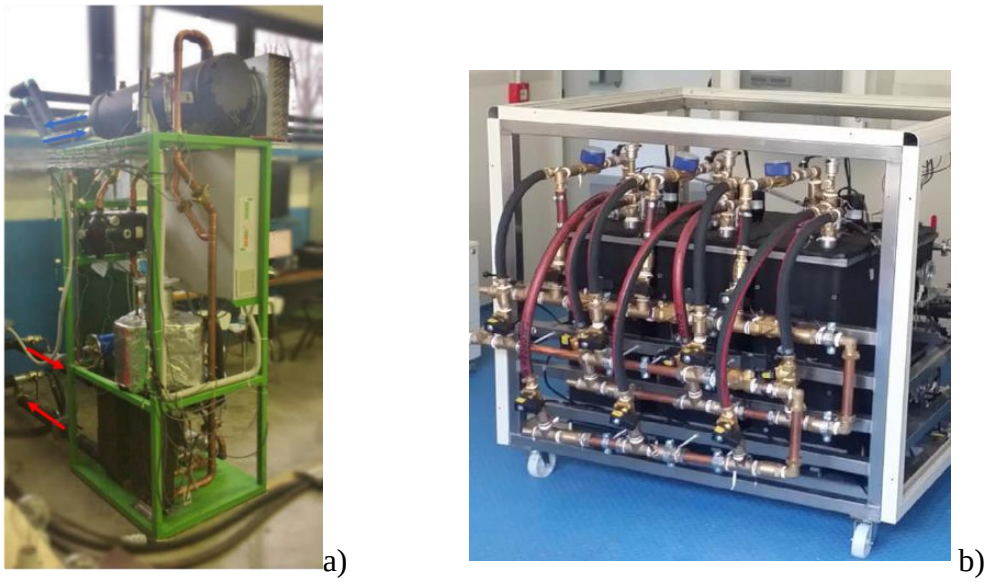

Figure 3. Views of (a) the ORC prototype, (b) AC prototype [22]

2. SIMULATION MODEL DESCRIPTION

The CCHP plant and the building, described in the previous section, have been implemented in TRNSYS 18 dynamic simulation software [45], as shown in Fig. 4.

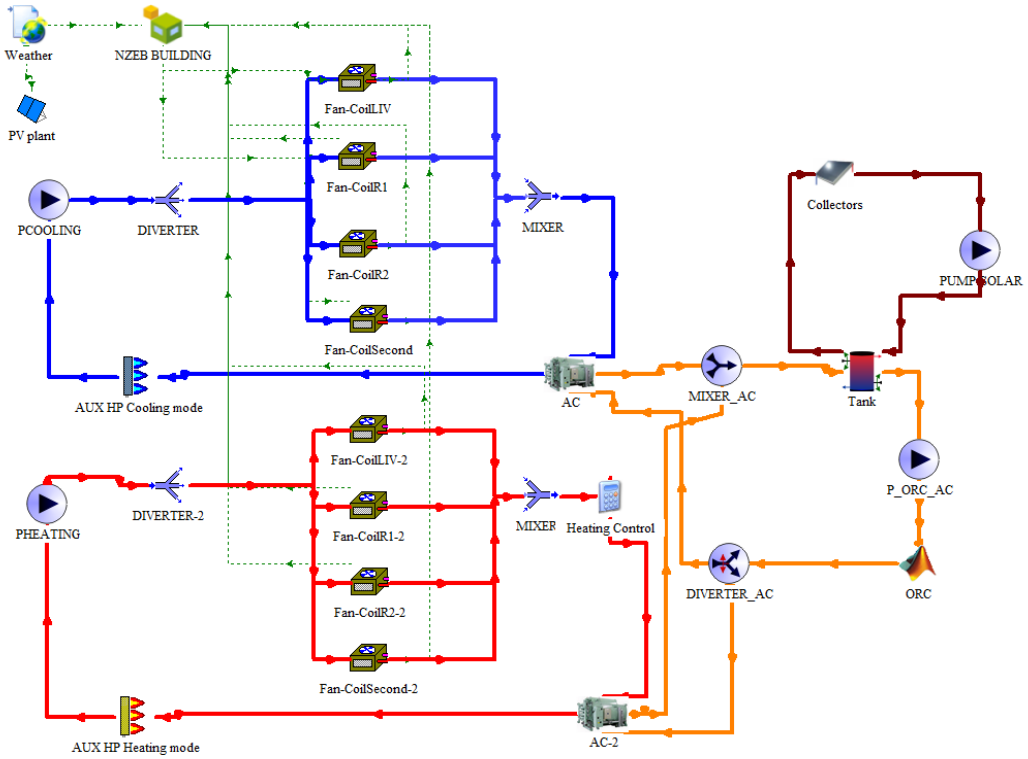

Figure 4. Scheme of the TRNSYS model

TRNSYS simulations are constructed by connecting individual component models (known as Types) together into a complete model. Many components of the CCHP system have been modelled

by means of existing Types from TRNSYS libraries while a specific subroutine for the ORC unit has been customized in Matlab [43]. The main components of the model are: Type 56 for the Building; Type 1b for the solar field; Type 194 for the PV plant; Type 4 for the Thermal Energy Storage (TES); Type 155 for calling Matlab subroutine; Type 909 for the adsorption chiller; Types 1246 and 659 for the Heat Pump during cooling and heating mode respectively; Type 600 for the Fan-coils. Types used for the model of ORC and AC units were modified with User-provide files that reply experimental performance data obtained by a full characterization of the real ORC and AC prototypes, at University of Bologna and at CNR - ITAE respectively. Weather data in terms of solar radiation and ambient temperature have been taken from Meteonorm database [44] on an hourly basis.

2.1 Building model (type 56)

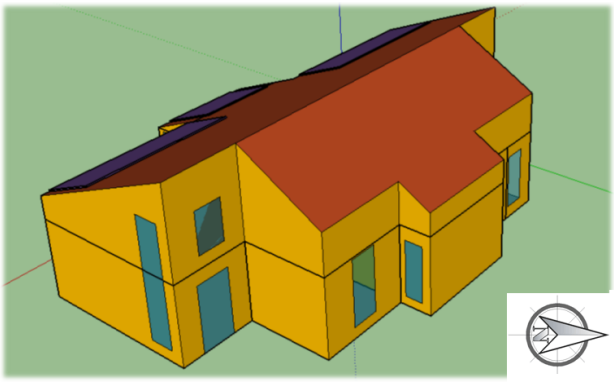

Figure 5. Building 3D model

The building was realized by means of Trnsys3d for SketchUp [46] and imported as 3D model into the Type 56, as shown in Fig. 5.
The building volume was divided into four thermal zones according to classifications and requirements specified by the Standard UNI 10339 [47]. The Air Change Rate has been fixed to 0.5 h^{-1}, in order to guarantee the required comfort conditions fixed by the standard UNI EN 15251 [48]. The dwelling is occupied by a family with four people (two working adults and two young students). Standardized factors of ASHRAE Standard 90.1-2004 have been used for occupancy and plug-loads that were modelled with typical schedules for residential kind of use [49]. LED lamps (50–90 lm/W) have been chosen to model light equipment. Indeed, an hydronic air-conditioning system have been chosen, according to TABULA WebTool [50] reporting the most diffused technologies in the last years used in residential buildings. Type 600 have been used to model 2-pipe fan coils able to deliver heating and cooling energy to the air stream inside the building.
The building performances have been simulated in Messina, Rome and Milan. These cities are characterized by different climatic conditions well representing the variability of Italian climates. Weather data and reference heating periods for each location are showed in Table 6.
During the winter, the heating set point temperature is 20 °C with an Upper dead band of 2 °C and a Lower dead band of -0.5 °C. The daily heating schedule is characterized by the reference zone and in particular:
ZONE B: 8 hours from 8.00 to 10:00, from 17:00 to 23:00.
ZONE D: 12 hours from 8.00 to 14:00, from 17:00 to 23:00.
ZONE E: 14 hours from 8.00 to 16:00, from 17:00 to 23:00

Table 6. Weather data and reference heating periods for each location

Location	Messina	Rome	Milan
Minimum annual temperature [°C]	11.8	7.7	1.9
Maximum annual temperature [°C]	26.5	24.4	23.8
Mean annual temperature [°C]	18.5	15.7	13.1
Latitude	38°11'39"48 N	41°53′35″N	45°28′01″N
Longitude	15°33'1"80 E	12°28′58″E	9°11′24″E
Climatic Zone	B	D	E
Heating Period	1 December-31 March	1 November-15 April	15 October-15 April
Degree days	707	1415	2404

In summer, the house is cooled at 26 °C with an Upper dead band of 2 °C and a Lower dead band of -3 °C. The same daily schedule is considered for all locations because a reference daily cooling period isn't defined by Italian law. Therefore, the dwelling is cooled from 8:00 to 20:00 every day during the cooling season.

2.2 CCHP model

Type 1 models a flat plate solar thermal collector using a quadratic efficiency equation from the well-known Hottel-Whillier equation:

$$\eta_{FPC} = a_0 - a_1 \frac{(\Delta T)}{I_T} - a_2 \frac{(\Delta T)^2}{I_T} \quad (1)$$

where a_0, a_1 and a_2 are three coefficients which depend on the type and model of the collectors; I_T is the Irradiation and ΔT is equal to the difference between the collector inlet temperature (T_i) and the ambient temperature (T_a).
The thermal power delivered to the fluid is described by Eq. (2):

$$Q_{FPC} = \dot{m}_{FPC} \cdot c_p \cdot \left(T_{FPC,out} - T_{FPC,in}\right) \quad (2)$$

The water flow rate of the solar circuit $\dot{m}_{FPC}$ has been set at 100 kg/h and the pump is controlled by a thermostat. The controller turns on the pump only when the outlet temperature from solar collectors ($T_{FPC,out}$) is higher than the average temperature of the TES (T_{TES}).
Photovoltaic panels have been modelled by means of Type 194 using parameters and reference conditions from commercial modules.
The ORC sub-model has been developed considering an empirical approach using empirical correlations derived from data obtained by experimental characterization. It performs basic balances for each iteration in order to obtain the power exchanged for each component. The thermodynamic properties of the working fluid in every section of the circuit are calculated by means of the open source CoolProp library [34] using temperature and pressure as input values.

The following assumptions have been considered for the ORC sub-model:

- heat losses at heat exchangers are neglected

- pressure losses along the circuit are neglected
- constant value of temperature difference at evaporator hot terminal (ΔT_{app})
- constant value of recuperator effectiveness (ε_{REC})
- constant value of pinch-point temperature difference at condenser (ΔT_{PP})
- constant value of expander electro-mechanical efficiency ($\eta_{m,el}$)

The assumption of a constant ΔT_{app} is justified by the high difference between the flow rates of organic fluid and hot water (which is at least one order of magnitude higher), resulting in a value of ΔT_{app} quite low and with little fluctuations; low variations have been observed also on recuperator effectiveness in most conditions during experiments; finally, the constant ΔT_{PP} value is consistent with experimental data in the range of operating conditions here analyzed.
The input variables depend on the operating conditions of the ORC system and of the cooling system and are:

- hot water temperature at the evaporator inlet, $T_{HW,I}$;
- cold water temperature at the condenser inlet, $T_{CW,I}$;
- hot and cold water flow rate, $\dot{V}_{HW}$, $\dot{V}_{CW}$
- superheating degree at expander inlet, ΔT_{SH}.

The input value of superheating degree is used to obtain the evaporation pressure of the cycle, according to Equation 3:

$$p_{ev} = p_{sat}(T_1 - \Delta T_{SH}) \tag{3}$$

where the saturation pressure is calculated via Coolprop and the difference $T_1 - \Delta T_{SH}$ corresponds to the evaporation temperature. Superheating degree is a design variable, whose value should be taken low in order to exploit the whole available pressure difference, but high enough to avoid wet expansion problems. The working fluid mass flow rate is computed using an empirical correlation, reported in Equation 4, as function of the evaporation pressure.

$$\dot{m}_{ORC} = \frac{p_{ev} - a}{b} \tag{4}$$

where the empirical coefficients *a* and *b* have been obtained from experimental trend of mass flow rate. All the above-mentioned constant quantities are collected in Table 7.

Table 7. Constant parameters for ORC submodel

Parameter	Value
ΔT_{app}	2 °C
ε_{REC}	0.65
ΔT_{PP}	4 °C
ΔT_{SH}	3 °C
$\eta_{m,el}$	0.9
a	7.015
b	72.35

The expander thermodynamic power ($P_{t,exp}$) and the pump consumption (P_{Pump}) are calculated according to Eq. (5) and (6).

$$P_{t,\exp} = \dot{m}_{ORC} \cdot (h_1 - h_2) \quad (5)$$

$$P_{Pump} = \dot{m}_{ORC} \cdot (h_5 - h_4) \quad (6)$$

where h_n is the enthalpy at the point n of the cycle.

The net electric power produced is then obtained as the difference of the expander electrical power output ($P_{el,exp}$) and the pump electric consumption ($P_{el,Pump}$) and is expressed by Eq. (7):

$$P_{el,ORC} = P_{el,\exp} - P_{el,Pump} = P_{t,\exp} \cdot \eta_{m,el} - P_{Pump} / \eta_{m,el} \quad (7)$$

Where $\eta_{m,el}$ is the electro-mechanical efficiency.

The adsorption chiller has been modelled using Type 909 relying on user-provided performance data files obtained in a previous full characterization of the prototype carried out at ITAE labs. A specific test bench has been devoted for thermally driven chillers and results highlighted the influence of the temperature difference between condenser (T_M) and evaporator (T_L) on the overall performance of the chiller. An average cooling power (ACP) between 3.4 and 4.4 kW, and a volumetric cooling power (VCP) of 7.25–9.36 kW/m^3, with a COP of 0.3–0.35, have been calculated from results at working conditions of T_H = 90 °C, T_L = 15÷18 °C and T_M = 25÷28 °C [36]. Thus, normalized capacity and COP ratios of the Type have been obtained as a function of the hot water inlet temperature, the cooling water inlet temperature and the chilled water inlet temperature.
The cooling power delivered from the chiller is equal to Eq. (8):

$$Q_c = COP_c \cdot Q_H \quad (8)$$

where COP_c is the coefficient of performance at current conditions during the cooling season and Q_H is the energy provided to the chiller by the inlet hot water flow stream.
The heating power delivered from the chiller is equal to Eq. (9):

$$Q_h = COP_h \cdot Q_H \quad (9)$$

where COP_h is the coefficient of performance at current conditions during the heating season.
The outlet water temperature to fan coils has been fixed at 40°C during the hot season varying the chilled water mass flow rate as a function of the COP and the inlet cooling temperature from fan coils.

3. RESULTS

The most representative results obtained from the simulations are presented in this section. The performance of the plants have been evaluated in terms of electric and thermal energy production on a monthly and yearly basis.

3.1 Thermal and electric loads

The building has been simulated in Messina, Rome and Milan. These cities are characterized by different climatic conditions and, thus, there is a high variability of thermal and cooling loads for

each location. Fig. 6 shows that the cooling energy demand of the building located in Messina is significantly higher than the other cities because of the high value of irradiation during summer period. On the contrary, due to the longest heating period and the lowest mean temperatures, the building located in Milan has the highest value of annual heating demand.
The base load of energy demand is covered by the AC unit while the peak of the load profile is delivered by the reversible HP. The CCHP system located in Messina covers almost completely the small heating demand but only the 35% of the cooling demand. The HP and AC working hours for Messina result comparable during the whole year and it is evident the AC results undersized. In Rome, the AC unit covers the 94% and 44% of the heating and cooling demand respectively. Finally, in Milan, the auxiliary HP covers only peaks of load profile during the coldest months while, in summer, the AC covers the entire cooling load. A summary of annual Heating and Cooling energy demand for each location is reported in Table 8.

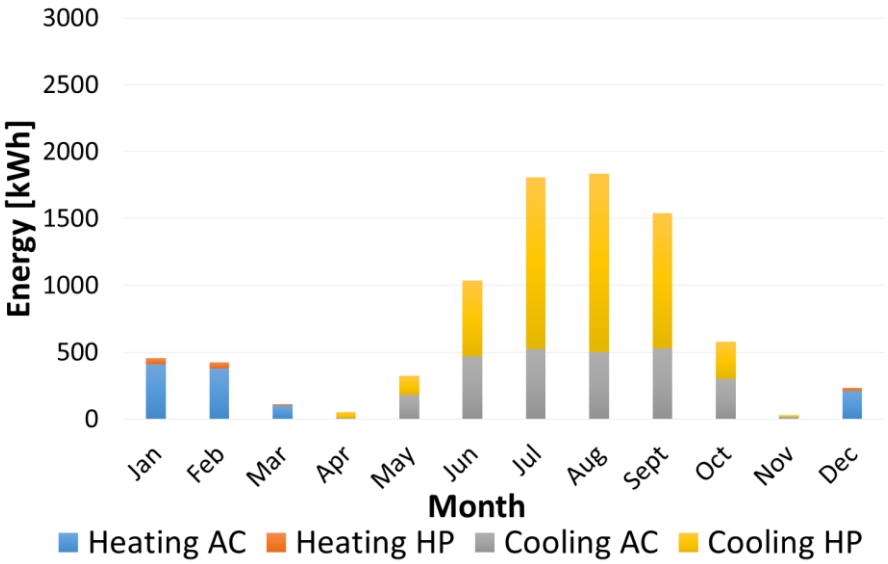

a)

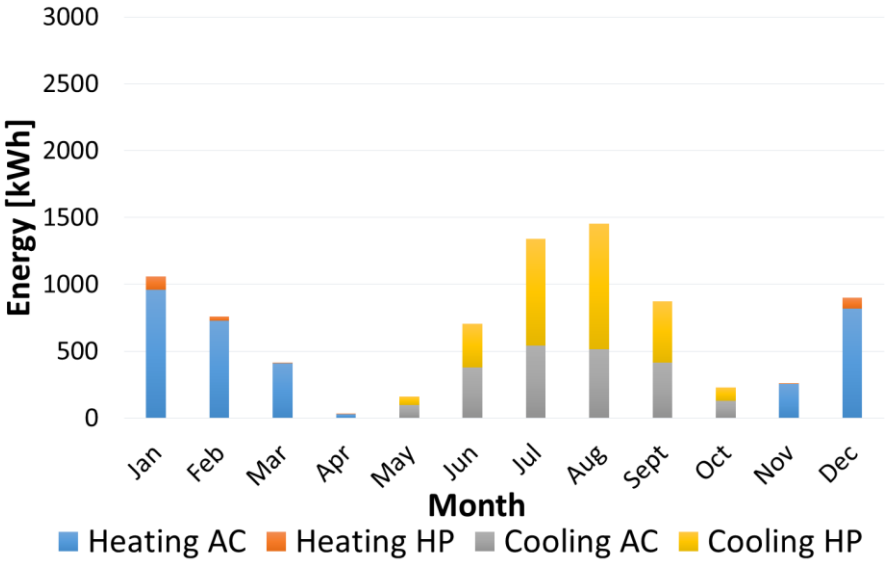

b)

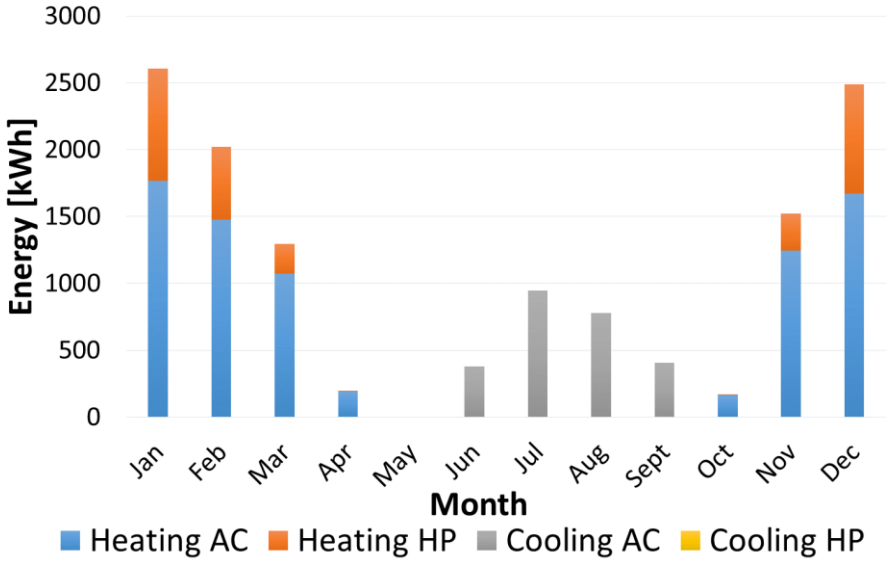

c)

Figure 6. Monthly distribution of Heating and Cooling energy demand for a) Messina b) Rome and c) Milan

Table 8. Summary of Heating and Cooling energy demand on annual basis for different locations

	Messina	Rome	Milan
Total Heating Energy [kWh$_h$]	1222	3415	10281
AC Heating Energy [kWh$_h$]	1100	3197	7581
HP Heating Energy [kWh$_h$]	122	218	2700
Total Cooling Energy [kWh$_c$]	7163	4757	2503
AC Cooling Energy [kWh$_c$]	2520	2073	2503
HP Cooling Energy [kWh$_c$]	4643	2684	0
h_{AC}	2246	2366	2603
h_{HP}	2113	1532	940

Fig. 7a-c and Fig. 8a-c report the following daily performance trends in winter and summer season respectively: the amount of solar radiation incident upon the total collector area (I_{tot}); the output thermal power delivered from the Flate Plate Collectors (Q_FPC); the auxiliary thermal power delivered to the TES from the electric resistances (Q_TES_aux); the input thermal power to supply the ORC (Q_ORC_in); the input thermal power to supply the AC (Q_AC_in); the output electric power produced by the ORC (P_ORC_el). During the heating period, the typical winter day considered in Fig. 7 shows that the input solar power is not enough to supply the CCHP and there is a high amount of backup energy during working hours. The load profile depends on the location and, thus, from the heating schedule of each climatic zone. For the city of Messina, the CCHP plant is turned off during the night and works mostly in the late afternoon. Fig 7.b shows the working strategy of the CCHP plant and the control unit turns off the ORC according to the building thermal load profile. On the contrary, in Milan, the heating request is high and quite constant during the day as shown in Fig.7c. In the last case, the most of all energy request is obtained from conversion of PV electrical energy in thermal energy to charge the TES. In summer, as shown in Fig. 8, for Rome and Messina, the solar energy production is higher and capable to deliver a consistent fraction of the energy required by CCHP system ranging from the 36% and 42%. In Milan, this fraction is about the 14% due to a lower irradiation. During cooling

season, the CCHP works all day long in all three cities and turned off in the night. In all configurations, the net ORC electric power is about 1.2 kW_e because supplied from the TES at a fixed temperature of 68°C.

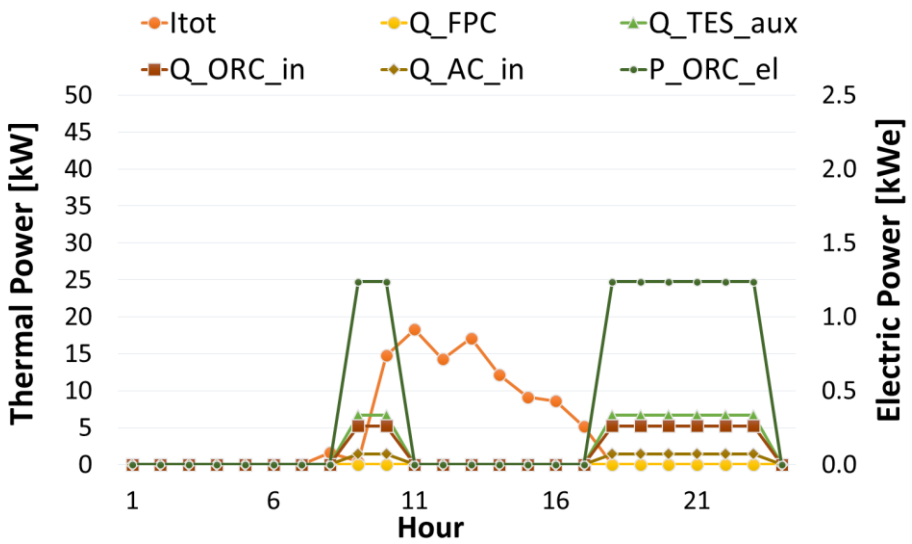

a)

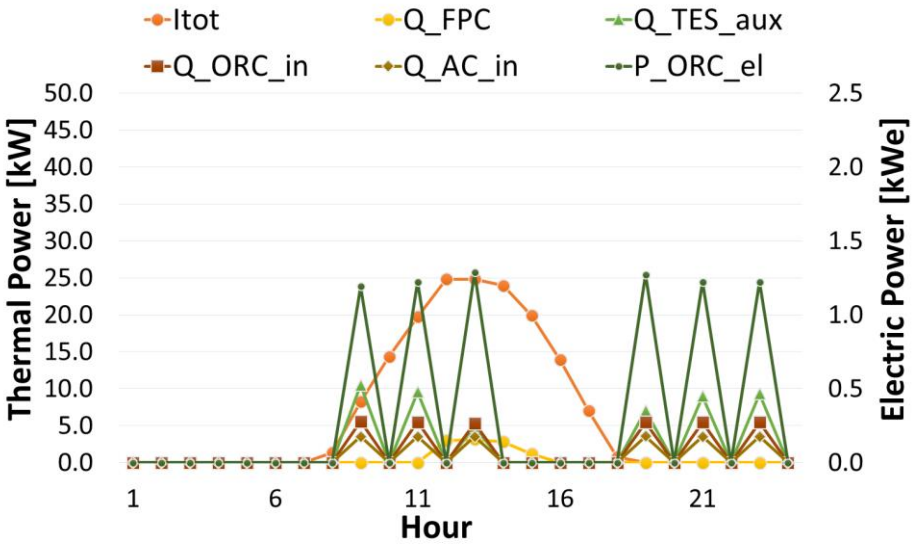

b)

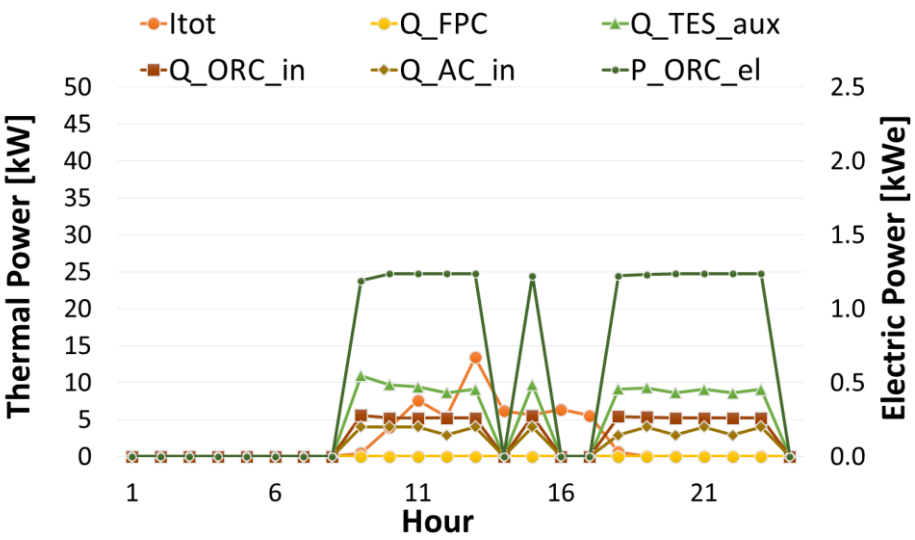

c)

Figure 7. Daily trend of the plant performances for a typical winter day a) in Messina b) in Rome and c) in Milan

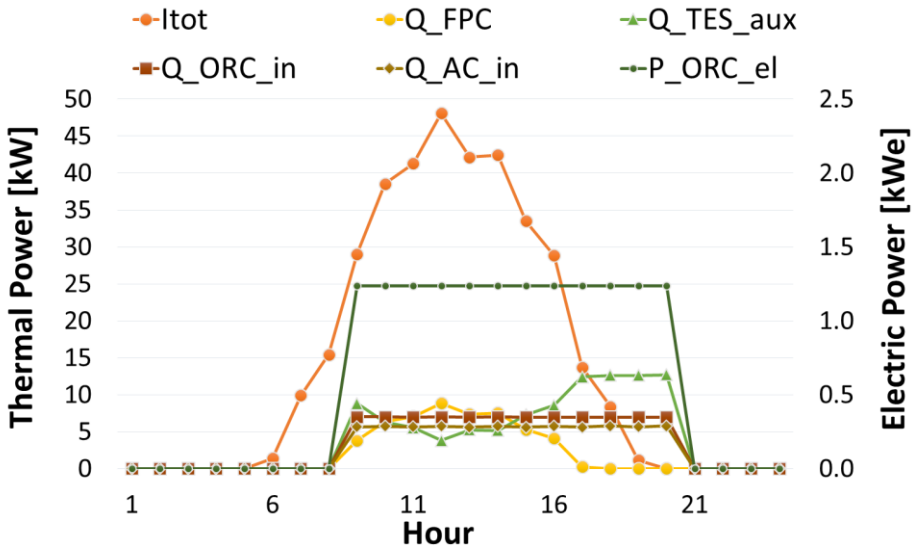

a)

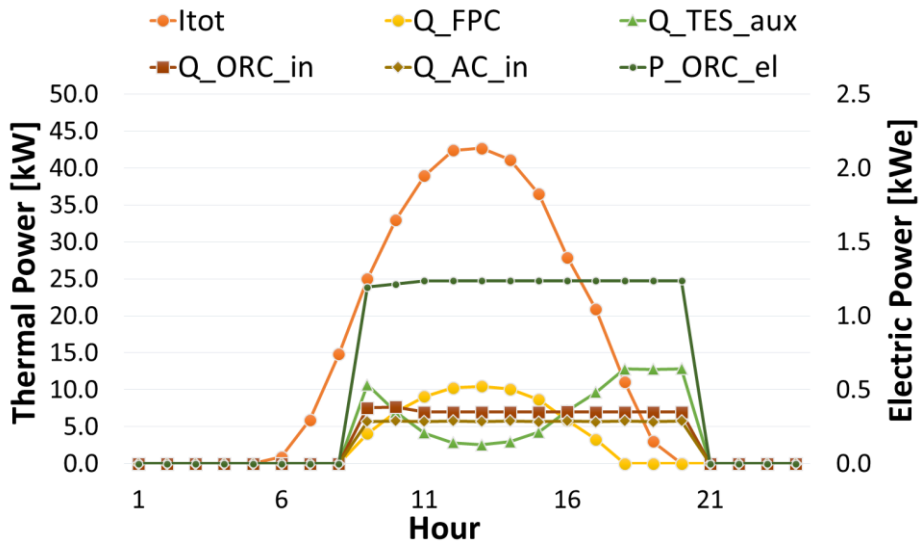

b)

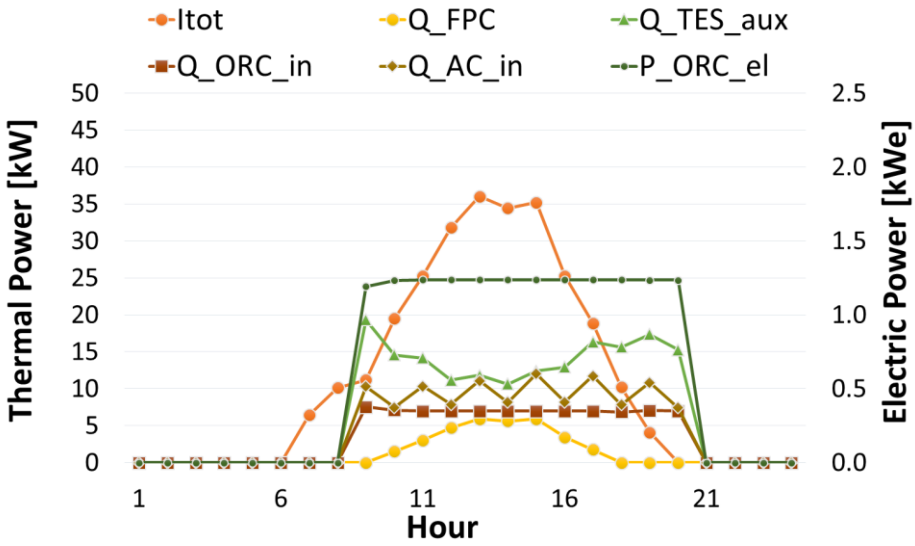

c)

Figure 8. Daily trend of the plant performances for a typical summer day a) in Messina b) in Rome and c) in Milan

The electrical balance of the entire system for each location is shown in Fig. 9 and summarized in Table 9. The building load is quite constant all over the year and covered for the 16% by the ORC electric energy production. This fraction can be increased using different management strategies of the CCHP. The rest of the electric load, composed by the electrical energy consumed by resistances of the TES and the auxiliary HP electric energy, is covered by the PV production and the electric energy imported from the Grid. For the city of Milan, the PV plant results undersized due to the lower irradiation thus a high amount of electricity is imported from the grid; however, the self-consumption index results the highest with a value of 58%. In the middle seasons, when the CCHP is turned off because there is no thermal load, the surplus of the PV production is fed into the grid.

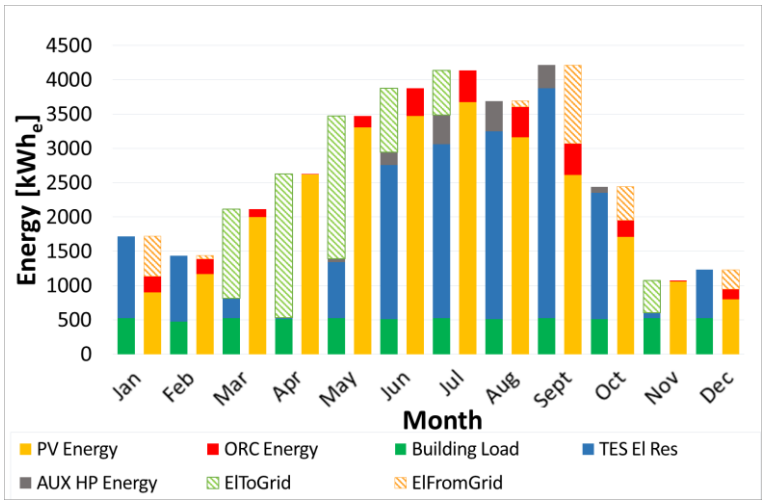

a)

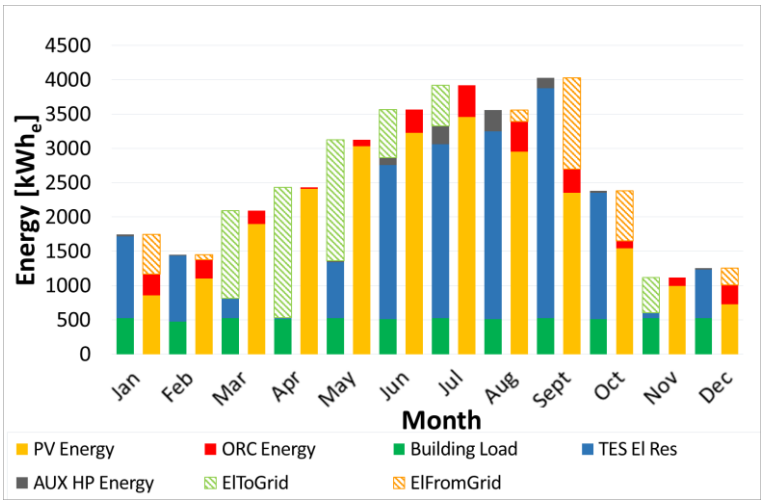

b)

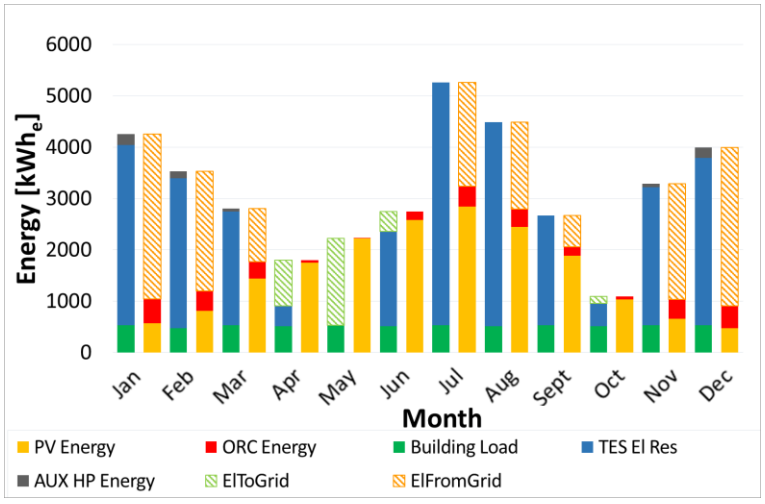

c)

Figure 9. Electrical Energy contributions for a) Messina b) Rome and c) Milan on monthly basis

Table 9. Electrical performances on annual basis for different locations

	Messina	Rome	Milan
Building load [kWh_e]	6203	6203	6203
HP Electrical Energy [kWh_e]	1579	950	940
TES Backup Electrical Energy [kWh_e]	16753	18888	28104
PV Electrical Energy [kWh_e]	26480	24547	18674
ORC Electrical Energy [kWh_e]	1069	1059	1071
Electric Energy from the Grid [kWh_e]	12862	14285	21590
Electric Energy to the Grid [kWh_e]	17762	15842	9162
Self-consumption index	40%	42%	58%

In order to compare the performances of the proposed CCHP system, efficiencies of the main components are reported in Table 10.
Also the global efficiency of the system ($\eta_{global,CCHP}$) is defined as the ratio between the useful electric, thermal, cooling energy and the inlet thermal energy from the solar field and the auxiliary energy:

$$\eta_{global,CCHP} = \frac{E_{heating} + E_{cooling} + E_{el,ORC}}{E_{FPC} + E_{el,HP} + E_{el,TES}} \quad (10)$$

Table 10. Global CCHP performances on annual basis for different locations

	Messina	Rome	Milan
η_{FPC}	11%	10%	7%
Seasonal $COP_{h,AC}$	1.3	1.3	1.3
Seasonal $COP_{c,AC}$	0.26	0.26	0.26
$\eta_{ORC,el}$	7%	7%	7%
$\eta_{global,CCHP}$	32%	32%	42%

The results have been compared to similar studies. Cioccolanti et al. proposed an experimental small scale prototype system composed of a 50m^2 CPC solar field, a 3.5 kWe ORC plantand a 17 kWc absorption chiller in [51]. Results showed a global efficiency value of 24.4% and the ORC unit reaches a mean electric efficiency of 4% during the whole year and a value of operating working hour limited to 650h due to a the limited area of the collectors of 50 m^2. Calise et al. designed and simulated a prototype of a small-scale solar CHP system based on evacuated flat-plate solar collectors and Organic Rankine Cycle and an average electric efficiency of 10% was found for the ORC. [52]. They can be comparable and show an energy performances similar to this case study.

3.2 Energy and environmental analysis

The energy, environmental and economic performance of proposed system are compared with those achieved by the reference system based on separated energy production. In the reference

system, the electric, cooling, and heating demand of the buildings are satisfied by the local electric grid, AC a compression chiller with a COP_c of 3.0, and gas fired boiler with a thermal efficiency of 0.92, respectively. The average Italian efficiency of thermo-electric power plant mix is equal to 0.44.

The primary energy savings of the overall system:

$$PES = \frac{PE_{ref} - PE_{CCHP}}{PE_{ref}} \tag{11}$$

Where the primary energy consumed by the reference system is:

$$PE_{ref} = PE_{heat} + PE_{cool} + PE_{FromGrid} = \frac{E_{heat}}{\eta_{boiler}} + \frac{E_{cool}}{EER_{ref} \cdot \eta_{Grid}} + \frac{E_{el,load}}{\eta_{Grid}} \tag{12}$$

The primary energy consumed by the simulated CCHP system is:

$$PE_{CCHP} = PE_{FromGrid} - PE_{ToGrid} = \frac{E_{FromGrid}}{\eta_{Grid}} - \frac{E_{ToGrid}}{\eta_{Grid}} \tag{13}$$

In Eq. (11) and (12), $PE_{FromGrid}$ represents the primary electric energy withdrawn from the grid, while, in equation (12) in case of insufficient electric production, PE_{ToGrid} represents the electric energy fed to the electric grid, in case of overproduction.
The environmental performance of the CCHP system is evaluated on the basis of on the equivalent dioxide emissions reduction ($CO_{2,avoided}$) respect to the reference system calculated in Eq. (14):

$$CO_{2,avoided} = f_{CO_2} \cdot (PE_{ref} - PE_{CCHP}) \tag{14}$$

Where f_{CO2}, the Italian CO_2 emission factor, is set at 0.39 kg_{CO2}/kWh [53].

Table 11. Energy and environmental analysis of CCHP, for different locations

Location	PES	$CO_{2,avoided}$
Messina	1.53	11713 kg_{CO2}
Rome	1.16	9213 kg_{CO2}
Milan	-0.01	-73 kg_{CO2}

In particular, the PES is negative for Milan. Due to a lower Irradiation, the electric energy production is not enough to feed the auxiliary heat pump for covering the heating demand and, thus, the PV plant results undersized.

3.3 Economic analysis

In this section the energy, environmental and economic results as well as the sensitivity analysis are presented.
The initial investment cost related to CCHP plant (IC_{CCHP}) is calculated summing the cost of all main components of the system, Furthermore, an installation cost of 15% has been taken into account. All specific costs have been taken from literature and the breakdown of the costs is showed in Table 12.

Unitary price of electric energy of 0.19 EUR/kWh$_e$ and of natural gas of 0.80 EUR/Sm^3 were considered as average seasonal values in Italy and were used to calculate the economic annual cost of the reference system.
The Electricity is exchanged with the grid by means of a specific feed-in policy mechanism ("Scambio Sul Posto", SSP) designed to provides economical compensation to PV system owners. Under SSP, the plant operator pays the supplier for the electricity consumed, while the Italian Electric Grid Manager (GSE) gives credit for the electricity fed in. The balance is calculated once a year and this method can lead to a surplus on behalf of the plant operator [54].

Table 12. Breakdown of the costs of the CCHP system

Component	Specific Cost	Total Cost
PV system	1700 EUR/kW	17000 EUR
Flat Plate Collectors	300 EUR/kW	18000 EUR
TES	2000 EUR	2000 EUR
Adsorption Chiller	1700 EUR/kW	7500 EUR
ORC	5000 EUR/kWe	15000 EUR
Heat Pump	6000 EUR	6000 EUR
Total sum		64000 EUR
Installation Cost		+15%
Total IC_{CCHP}		73500 EUR

The Net Present Value (NPV) has been calculated in order to analyze the profitability of the investment according to Eq. (15):

$$NPV = \sum_{k=0}^{n} \frac{F_k}{(1+i)^k} \tag{15}$$

Where F_k is the net cash inflow-outflows during a single period k, "i" is the discount rate of return fixed at 0.04, and n is the amount of years of the useful life of the plant.
Initially, the Simple Pay Back (SPB) has been evaluated without considering any type of incentives, in order to perform the economic analysis according to Eq. (16):

$$NPV = \sum_{k=0}^{SPB} \frac{F_k}{(1+i)^k} = 0 \tag{16}$$

Considering Table 13 and Eq. (17) a SPB of years has been obtained. This payback period is not acceptable. However, in Italy the economic feasibility of these systems is supported by economic incentives.
Thus the SPB_{inc} has been evaluated, taking into account an incentive about the covering of 65% of the initial investment cost related to the CCHP plant [55];

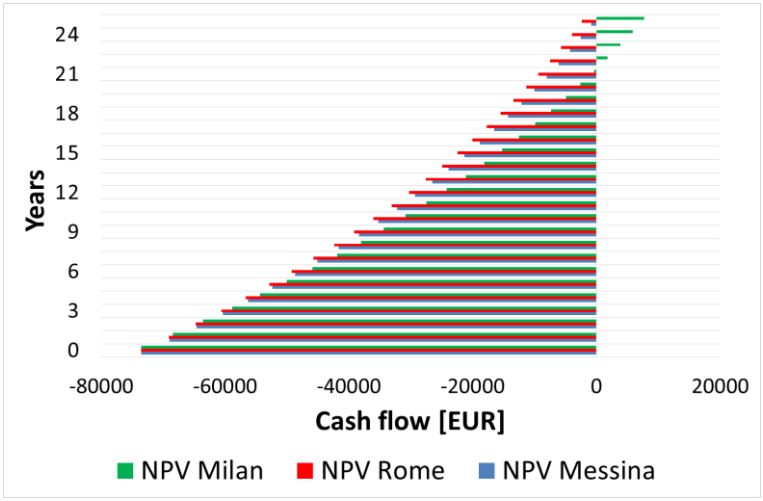

a)

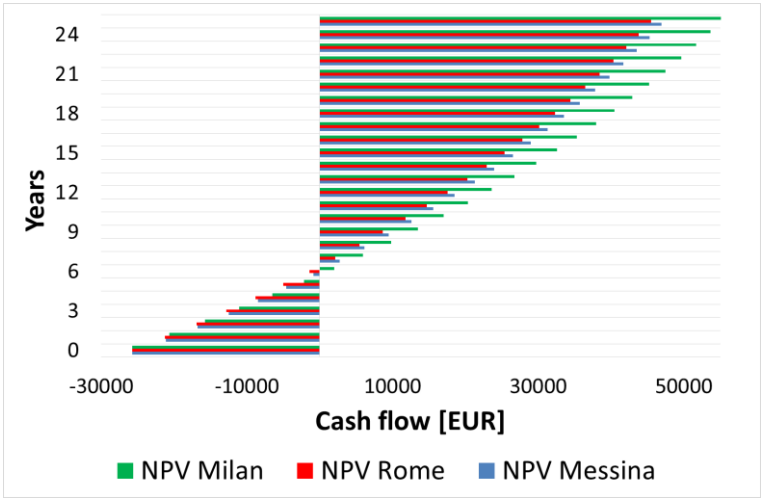

b)

Figure 12. NPV for different locations a) without incentives and b) with incentives

Table 13. Economic analysis of CCHP, for different locations without incentives and with incentives

Location	NPV (25 y)	SPB	NPV_{inc}	SPB_{inc}
Messina	-853 EUR	>25 y	47000 EUR	6 y
Rome	-2342 EUR	>25 y	45500 EUR	7 y
Milan	7750 EUR	22 y	55500 EUR	6 y

It's reasonable considering an economic feasibility with a SPB of 10 years. The minimum incentive to achieve this value is about the 50% of the initial investment cost. Thus, the CCHP feasibility can be evaluated also taking in account other values for nations with different economic support mechanisms.

The overall economic performances have been compared to other works as well as done in the energy analysis. Taking in account as reference systems the previous works [51,52], values of PBT results over 25 years and 13 years respectively. Considering a government's financial support, the PBT can achieve values of 13 years and 5 years for the considered configurations.

Therefore, it can be concluded that results above have been successfully validated on the basis of similar works available in literature.

CONCLUSIONS

In this work, a small scale solar CCHP system conceived for the residential sector has been investigated by means of a dynamic model in TRNSYS. The system is based on a 3 kW_e ORC and a 4.4 kW_c thermally driven Adsorption Chiller experimental prototypes and a solar field is supposed to be the primary source. Nevertheless the plant is able to work with any low temperature power supply. The water heated in the solar collectors is used to feed a 2 m^3 thermal energy storage used as heat buffer, which is provided with electro-resistances as supplementary thermal source to supply the ORC unit and in cascade, the adsorption chiller. The system is also equipped with an auxiliary 6 kW_c reversible heat pump to cover the peak of the thermal energy demand from the building. The main innovation of the model is the integration of the micro-ORC unit with the adsorption chiller, implemented on TRNSYS by user-defined types that use performance data obtained by a full experimental characterization of ORC and AC prototypes, which are installed and currently working at University of Bologna and at CNR - ITAE respectively. The dynamic performances of the considered system have been evaluated with respect to a real "nearly zero energy building" (NZEB) located in three different cities representative of the Italian climatic zones: Messina, Rome and Milan. Results of simulations, which have been carried out on hourly basis, revealed the great influence of solar radiation and weather conditions on the effectiveness of the system. The CCHP plant works for about 2400 hours per year on average with different load profiles and can achieve a global efficiency ranging between 32% and 42%.

A techno-economic analysis was carried out and the payback period of the analysed solution results more than 25 years unless economic support mechanisms are considered. If the initial cost is supported by economic incentives, the economic analysis shows that the proposed CCHP system can achieve a Pay Back Time of 6 years with a Net Present Value of 50 kEUR at 25 years. The economic feasibility of the CCHP system can be achieved also for different government's financial supports considering a minimum economic incentive of 50% of the initial investment cost.

In conclusion, this study has highlighted the potential of solar driven micro-CCHP systems for residential applications, and its economic feasibility if government's financial support is available; moreover, the proposed model can be adopted as a tool for the design of similar systems by redefining the different subsystems according to the desired technology.

Future activities will be dedicated to validation of the proposed model by means of a lab-scale installation at the CNR ITAE labs. Also, many strategies of optimization of the studied CCHP system will be analyzed to achieve better performances.

REFERENCES

[1] IEA, Energy Efficiency indicators (database), (2017).

[2] Eurostat, Energy Balance, (2017). http://ec.europa.eu/eurostat/web/energy/data/energy-balances.

[3] Directive 2010/31/EU of the European Parliament and of Council of 19 May 2010 on the energy performance of buildings (recast), Off. J. Eur. Union. (2010) 13–25.

[4] F. Ascione, R.F. De Masi, F. de Rossi, S. Ruggiero, G.P. Vanoli, Optimization of building envelope design for nZEBs in Mediterranean climate: Performance analysis of residential case study, Appl. Energy. 183 (2016) 938–957.

https://doi.org/10.1016/j.apenergy.2016.09.027.
[5] D. D'Agostino, D. Parker, A framework for the cost-optimal design of nearly zero energy buildings (NZEBs) in representative climates across Europe, Energy. 149 (2018) 814–829. https://doi.org/10.1016/j.energy.2018.02.020.
[6] G. Tumminia, F. Guarino, S. Longo, D. Aloisio, S. Cellura, F. Sergi, G. Brunaccini, V. Antonucci, M. Ferraro, Grid interaction and environmental impact of a net zero energy building, Energy Convers. Manag. 203 (2020). https://doi.org/10.1016/j.enconman.2019.112228.
[7] S. Deng, A. Dalibard, M. Martin, U. Eicker, Energy supply concepts for zero energy residential buildings in humid and dry climate, Energy Convers. Manag. 52 (2011) 2455–2460. https://doi.org/10.1016/J.ENCONMAN.2010.12.054.
[8] M. Ebrahimi, A. Keshavarz, CCHP Literature, in: Comb. Cool. Heat. Power, 2015: pp. 1–34. https://doi.org/10.1016/b978-0-08-099985-2.00001-9.
[9] M. Bianchi, A. De Pascale, P.R. Spina, Guidelines for residential micro-CHP systems design, Appl. Energy. 97 (2012) 673–685. https://doi.org/10.1016/j.apenergy.2011.11.023.
[10] M.M. Maghanki, B. Ghobadian, G. Najafi, R.J. Galogah, Micro combined heat and power (MCHP) technologies and applications, Renew. Sustain. Energy Rev. 28 (2013) 510–524. https://doi.org/10.1016/j.rser.2013.07.053.
[11] A. Akisawa, T. Miyazaki, T. Kashiwagi, Theoretical analysis of the optimal configuration of co-generation systems and competitiveness of heating/cooling technologies, Energy. 35 (2010) 4071–4078. https://doi.org/10.1016/j.energy.2010.06.015.
[12] E. Cardona, A. Piacentino, F. Cardona, Matching economical, energetic and environmental benefits: An analysis for hybrid CHCP-heat pump systems, Energy Convers. Manag. 47 (2006) 3530–3542. https://doi.org/10.1016/j.enconman.2006.02.027.
[13] G. Angrisani, A. Akisawa, E. Marrasso, C. Roselli, M. Sasso, Performance assessment of cogeneration and trigeneration systems for small scale applications, Energy Convers. Manag. 125 (2016) 194–208. https://doi.org/10.1016/j.enconman.2016.03.092.
[14] V. Zare, H. Rostamnejad Takleh, Novel geothermal driven CCHP systems integrating ejector transcritical CO2 and Rankine cycles: Thermodynamic modeling and parametric study, Energy Convers. Manag. 205 (2020) 112396. https://doi.org/10.1016/J.ENCONMAN.2019.112396.
[15] D. Wu, J. Zuo, Z. Liu, Z. Han, Y. Zhang, Q. Wang, P. Li, Thermodynamic analyses and optimization of a novel CCHP system integrated organic Rankine cycle and solar thermal utilization, Energy Convers. Manag. 196 (2019) 453–466. https://doi.org/10.1016/J.ENCONMAN.2019.06.020.
[16] J.S. Pereira, J.B. Ribeiro, R. Mendes, G.C. Vaz, J.C. André, ORC based micro-cogeneration systems for residential application - A state of the art review and current challenges, Renew. Sustain. Energy Rev. 92 (2018) 728–743. https://doi.org/10.1016/j.rser.2018.04.039.
[17] I. Garcia-Saez, J. Méndez, C. Ortiz, D. Loncar, J.A. Becerra, R. Chacartegui, Energy and economic assessment of solar Organic Rankine Cycle for combined heat and power generation in residential applications, Renew. Energy. 140 (2019) 461–476. https://doi.org/10.1016/j.renene.2019.03.033.
[18] G. Angrisani, C. Roselli, M. Sasso, F. Tariello, Dynamic performance assessment of a micro-trigeneration system with a desiccant-based air handling unit in Southern Italy climatic conditions, Energy Convers. Manag. 80 (2014) 188–201. https://doi.org/10.1016/j.enconman.2014.01.028.
[19] R.Z. Wang, R.G. Oliveira, Adsorption refrigeration-An efficient way to make good use of waste heat and solar energy, Prog. Energy Combust. Sci. 32 (2006) 424–458. https://doi.org/10.1016/j.pecs.2006.01.002.

[20] G. Santori, A. Sapienza, A. Freni, A dynamic multi-level model for adsorptive solar cooling, Renew. Energy. 43 (2012) 301–312. https://doi.org/10.1016/j.renene.2011.11.039.
[21] Z. Xia, D. Wang, J. Zhang, Experimental study on improved two-bed silica gel-water adsorption chiller, Energy Convers. Manag. 49 (2008) 1469–1479. https://doi.org/10.1016/j.enconman.2007.12.019.
[22] Z.S. Lu, R.Z. Wang, Z.Z. Xia, Q.B. Wu, Y.M. Sun, Z.Y. Chen, An analysis of the performance of a novel solar silica gel-water adsorption air conditioning, Appl. Therm. Eng. 31 (2011) 3636–3642. https://doi.org/10.1016/j.applthermaleng.2010.11.024.
[23] A. Freni, G. Maggio, A. Sapienza, A. Frazzica, G. Restuccia, S. Vasta, Comparative analysis of promising adsorbent/adsorbate pairs for adsorptive heat pumping, air conditioning and refrigeration, Appl. Therm. Eng. 104 (2016) 85–95. https://doi.org/https://doi.org/10.1016/j.applthermaleng.2016.05.036.
[24] S. Vasta, G. Giacoppo, O. Barbera, L. Calabrese, L. Bonaccorsi, A. Freni, Innovative zeolite coatings on graphite plates for advanced adsorbers, Appl. Therm. Eng. 72 (2014) 153–159. https://doi.org/https://doi.org/10.1016/j.applthermaleng.2014.04.079.
[25] V. Palomba, S. Vasta, A. Freni, Experimental testing of AQSOA FAM Z02/water adsorption system for heat and cold storage, Appl. Therm. Eng. 124 (2017) 967–974. https://doi.org/https://doi.org/10.1016/j.applthermaleng.2017.06.085.
[26] H. Wei Benjamin Teo, A. Chakraborty, W. Fan, Improved adsorption characteristics data for AQSOA types zeolites and water systems under static and dynamic conditions, Microporous Mesoporous Mater. 242 (2017) 109–117. https://doi.org/10.1016/j.micromeso.2017.01.015.
[27] K. Grabowska, J. Krzywanski, W. Nowak, M. Wesolowska, Construction of an innovative adsorbent bed configuration in the adsorption chiller - Selection criteria for effective sorbent-glue pair, Energy. 151 (2018) 317–323. https://doi.org/10.1016/j.energy.2018.03.060.
[28] A. Saeed, A. Al-Alili, A review on desiccant coated heat exchangers, Sci. Technol. Built Environ. 23 (2017) 136–150. https://doi.org/10.1080/23744731.2016.1226076.
[29] M. Verde, L. Cortés, J.M. Corberán, A. Sapienza, S. Vasta, G. Restuccia, Modelling of an adsorption system driven by engine waste heat for truck cabin A/C. Performance estimation for a standard driving cycle, Appl. Therm. Eng. 30 (2010) 1511–1522. https://doi.org/10.1016/j.applthermaleng.2010.04.005.
[30] S. Vasta, A. Freni, A. Sapienza, F. Costa, G. Restuccia, Development and lab-test of a mobile adsorption air-conditioner, Int. J. Refrig. 35 (2012) 701–708. https://doi.org/10.1016/j.ijrefrig.2011.03.013.
[31] InvenSor, (n.d.). https://invensor.com/en/home/.
[32] Fahrenheit, (n.d.). https://fahrenheit.cool/en/.
[33] M. Bianchi, L. Branchini, N. Casari, A. De Pascale, F. Melino, S. Ottaviano, M. Pinelli, P.R. Spina, A. Suman, Experimental analysis of a micro-ORC driven by piston expander for low-grade heat recovery, Appl. Therm. Eng. 148 (2019) 1278–1291. https://doi.org/10.1016/j.applthermaleng.2018.12.019.
[34] M. Bianchi, L. Branchini, A. De Pascale, F. Melino, S. Ottaviano, A. Peretto, N. Torricelli, Application and comparison of semi-empirical models for performance prediction of a kW-size reciprocating piston expander, Appl. Energy. 249 (2019) 143–156. https://doi.org/10.1016/j.apenergy.2019.04.070.
[35] M. Bianchi, L. Branchini, A. De Pascale, F. Melino, S. Ottaviano, A. Peretto, N. Torricelli, G. Zampieri, Performance and operation of micro-ORC energy system using geothermal heat source, Energy Procedia. 148 (2018) 384–393. https://doi.org/10.1016/j.egypro.2018.08.099.

[36] A. Sapienza, G. Gullì, L. Calabrese, V. Palomba, A. Frazzica, V. Brancato, D. La Rosa, S. Vasta, A. Freni, L. Bonaccorsi, G. Cacciola, An innovative adsorptive chiller prototype based on 3 hybrid coated/granular adsorbers, Appl. Energy. 179 (2016) 929–938. https://doi.org/10.1016/j.apenergy.2016.07.056.
[37] A. Sapienza, V. Palomba, G. Gullì, A. Frazzica, S. Vasta, A new management strategy based on the reallocation of ads-/desorption times: Experimental operation of a full-scale 3 beds adsorption chiller, Appl. Energy. 205 (2017) 1081–1090. https://doi.org/10.1016/j.apenergy.2017.08.036.
[38] W. Lombardo, S. Ottaviano, L. Branchini, S. Vasta, A. De Pascale, A. Sapienza, A dynamic model of a solar driven trigeneration system based on micro-ORC and adsorption chiller prototypes, in: AIP Conf. Proc., 2019. https://doi.org/10.1063/1.5138831.
[39] Decree 412/93, (n.d.). http://www.gazzettaufficiale.it/eli/id/1993/10/14/ 093G0451/sg.
[40] Segheria Vecchio s.n.c., (n.d.). https://www.segheriavecchio.it/case-blog/casa-mazza.
[41] G. Zampieri, CLOSED-CYCLE PLANT, 20,160,032,786, 2016.
[42] H. Kakiuchi, S. Shimooka, M. Iwade, K. Oshima, M. Yamazaki, S. Terada, H. Watanabe, T. Takewaki, Water vapor adsorbent FAM-Z02 and its applicability to adsorption heat pump, Kagaku Kogaku Ronbunshu. 31 (2005) 273–277. https://doi.org/10.1252/kakoronbunshu.31.273.
[43] Oker-Chemie GmbH, (n.d.). http://www.oker-chemie.de/pdfs/Mat_SIO_01_SW_englisch.pdf.
[44] G. Santori, A. Frazzica, A. Freni, M. Galieni, L. Bonaccorsi, F. Polonara, G. Restuccia, Optimization and testing on an adsorption dishwasher, Energy. 50 (2013) 170–176. https://doi.org/10.1016/J.ENERGY.2012.11.031.
[45] TRNSYS – Transient System Simulation Tool, (n.d.). http://www.trnsys.com/.
[46] SketchUp 3D design Software, (n.d.). https://www.sketchup.com/.
[47] UNI – Italian Committee for Standardization. Standard UNI 10339: Air conditioning systems for thermal comfort in buildings. General, classification and requirements. Offer, order and supply specifications, (1995).
[48] UNI – Italian Committee for Standardization. Standard UNI EN 15251: Indoor environmental input parameters for design and assessment of energy performance of buildings addressing indoor air quality, thermal environment, lighting and acoustics, (2008).
[49] American Society of Heating, Refrigerating and Air-Conditioning Engineers (ASHRAE) Standard 90.1-2004, (n.d.).
[50] TABULA WebTool, (2016). http://episcope.eu/building-typology/webtool.
[51] L. Cioccolanti, R. Tascioni, E. Bocci, M. Villarini, Parametric analysis of a solar Organic Rankine Cycle trigeneration system for residential applications, Energy Convers. Manag. 163 (2018) 407–419. https://doi.org/10.1016/j.enconman.2018.02.043.
[52] F. Calise, M.D. D'Accadia, M. Vicidomini, M. Scarpellino, Design and simulation of a prototype of a small-scale solar CHP system based on evacuated flat-plate solar collectors and Organic Rankine Cycle, Energy Convers. Manag. 90 (2015) 347–363. https://doi.org/10.1016/j.enconman.2014.11.014.
[53] IEA, Statistics, CO2 Emissions from Fuel Combustion, (2015).
[54] Scambio sul posto, (n.d.). https://www.gse.it/servizi-per-te/fotovoltaico/scambio-sul-posto.
[55] Conto termico, (n.d.). https://www.gse.it/servizi-per-te/efficienza-energetica/conto-termico.